Vapour - liquid Equilibrium and Thermodynamic Properties of Refrigerant R23 from Cubic Equations of State

MIRELA IONITA, VIOREL FEROIU*, DAN GEANA
Politehnica University Bucharest, Department of Applied Physical Chemistry and Electrochemistry, 1 Polizu Str., 011061, Bucharest, Romania

Vapour – liquid equilibrium and thermodynamic properties were predicted, along the saturation curve and in the single-phase region for refrigerants R23 (CHF_3). Five cubic equations of state were used: Soave-Redlich-Kwong (SRK), Peng-Robinson (PR), Trebble-Bishnoi-Salim (TBS), Freze et al (C1), and GEOS3C. A wide comparison with recommended NIST (National Institute of Standard and Technology, USA) data, considered as pseudo-experimental data was made. This study shows that the cubic EOSs lead to reasonable predictions of thermodynamic properties of refrigerant R23, resting simple enough for applications. The GEOS3C equation has some advantages, notably being a general form for all the cubic equations of state with two, three and four parameters proposed in the literature. A slightly modification of the temperature function in its cohesive term solves the problem of discontinuity in some thermodynamic properties at critical temperature of the pure fluids.

Keywords: *equation of state, vapour - liquid equilibrium, thermodynamic properties, refrigerants*

Refrigerants are the working fluids in refrigeration, air-conditioning and heat pumping systems. They absorb heat from one area, such as an air-conditioned space, and reject it into another, such as outdoors, usually through evaporation and condensation, respectively. A refrigerant must satisfy many requirements: chemical stability, transfer heat ability, low toxicity, efficiency, reduced environmental consequences. Chemical stability under conditions of use is the most important characteristic. No single fluid satisfies all the attributes desired of a refrigerant, and as a result, a variety of refrigerants is used. Refrigerant selection involves compromises between conflicting desirable thermodynamic properties.

In the classical thermodynamic framework it is possible to develop relations to calculate the Helmholz and Gibbs energies, enthalpies, entropies, fugacity coefficients and other thermodynamic properties of fluids. Such relationships together with equations of states can be applied to obtain estimation techniques for thermodynamic property departure functions [1]. Then the "true" thermodynamic properties are calculated for pure components and mixtures.

The equations of state (EOSs) models are the most common approach for the correlation and prediction of phase equilibria and thermodynamic properties of the fluids and fluid mixtures. The advances in developing cubic EOS models, with different complexities, are listed in several reviews [2-4]. Polishuk et al [5, 6] analyzed the advantages and limitations of cubic EOSs for simultaneous prediction of the critical and sub-critical phase behaviour in mixtures.

In the last decades, a progress has been made in implementing molecular theories, as the Statistical Association Fluid Theory (SAFT) of Wertheim [7, 8], in equations of state. The first developments are the SAFT equation of state of Chapman et al [9, 10], and the CPA (Cubic Plus Association) of Kontogeorgis et al [11], followed by other models. The comprehensive reviews of different SAFT EOS models are available elsewhere [12, 13]. This statistical theory became very popular because it offers a relationship between atomic and macroscopic scales of pure substances and mixtures.

But these SAFT-type models also exhibit some weaknesses, notably are not able to provide a good representation of pure component and mixture critical properties. Recently, Polishuk [14] demonstrated that the SAFT EOS models might exhibit unrealistic and even non-physical predictions as negative heat capacities, intersections of isotherms at high pressures, additional critical points and fictive phase equilibria. Privat et al [15] have shown that for pure fluids at a fixed temperature and pressure, these equations of state exhibit up to five molar volumes, leading to the simultaneous existence of pseudo liquid–liquid and liquid–vapour phase equilibria at a same temperature, or the presence of a liquid–liquid azeotrope.

In spite of these new developments, cubic EOSs remain important and easy tools to calculate the phase behaviour in many systems, even for complex mixtures like petroleum fluids [16-18]. Moreover, cubic EOSs can be integrated in semiempirical hybrid model, as PHSGEOS [19] and SAFT + Cubic EOS [20], by combining the non-association terms of SAFT with a cohesive cubic term.

The trifluoromethane (R23) is an environmentally acceptable refrigerant and of interest in the application for alternative refrigerants. The purpose of this work is to present the result of vapour – liquid equilibrium (VLE), volumetric and thermodynamic properties prediction of R23 pure fluid, and to compare the results with recommended NIST (National Institute of Standard and Technology, USA) data [21], considered as pseudo-experimental data.

Taking into account the above considerations, we decided to model the behaviour of refrigerant R23, along the saturation curve and in the single-phase region with five cubic equations of state: Soave-Redlich-Kwong (SRK) [22], Peng-Robinson (PR) [23], Trebble-Bishnoi-Salim (TBS) [24], Freze et al (C1) [25], and GEOS3C [26].

This study shows that the cubic EOSs lead to reasonable predictions of VLE and thermodynamic properties of R23, resting simple enough for applications in chemical

* *email: v_feroiu@chim.upb.ro; Tel: +4021 4023988*

engineering. The GEOS3C equation has some advantages, notably being a general form for all the cubic equations of state with two, three and four parameters proposed in the literature. A slightly modification of the temperature function in its cohesive term solves the problem of discontinuity in some thermodynamic properties at critical temperature of the pure fluids.

Modeling

The general cubic equation of state (GEOS3C) has the form:

$$P = \frac{RT}{V-b} - \frac{a(T)}{(V-d)^2+c} \quad (1)$$

The four parameters a, b, c, d for a pure component are expressed by:

$$a(T) = a_c\,\beta(T_r); \quad a_c = \Omega_a \frac{R^2T_c^2}{P_c}; \quad b = \Omega_b \frac{RT_c}{P_c};$$
$$c = \Omega_c \frac{R^2T_c^2}{P_c^2}; \quad d = \Omega_d \frac{RT_c}{P_c}; \quad (2)$$

The GEOS3C equation uses the temperature function in the cohesive term $a(T)$[26]:

$$\beta(T_r) = (1 + C_1 y + C_2 y^2 + C_3 y^3)^2 \quad \text{for } T_r \le 1, \quad (3)$$
$$\beta(T_r) = (1 + C_1 y)^2 \quad \text{for } T_r > 1 \quad (4)$$

$y = 1 - \sqrt{T_r}$ with the reduced temperature $T_r = T / T_c$.

The temperature function (3-4) as well as its first derivative are continuous in the critical point. The second derivative is not continuous, and this fact leads to a discontinuity in the isochoric and isobaric heat capacities and other properties involving the second derivative, at the critical point. In order to avoid this discontinuity we suggested a modification of the temperature function [27], by using the eq. (3) on the entire T_r range:

$$\beta(T_r) = (1 + C_1 y + C_2 y^2 + C_3 y^3)^2 \quad \text{for } \forall\ T_r \quad (5)$$

The second derivative discontinuity has an effect on the isochoric and isobaric heat capacities as can be seen from the following equations [1]:

$$\Delta C_V^R = \left[\frac{\partial(\Delta U^R)}{\partial T}\right]_V = T\frac{\partial^2 a}{\partial T^2}E \quad (6)$$

$$\Delta C_P^R = \Delta C_V^R - T\frac{(\partial P/\partial T)_V^2}{(\partial P/\partial V)_T} - R \quad (7)$$

with

$$E = \frac{1}{2\sqrt{-c}}\ln\frac{V-d+\sqrt{-c}}{V-d-\sqrt{-c}} \quad \text{for } c<0 \quad (8)$$

Moreover, the new temperature function (5) has the important advantage to not involve a reoptimization of C_1, C_2, C_3 parameters of GEOS3C equation, the available values in the literature [26] being used to predict the thermodynamic properties of pure components with the modified temperature function.

The expressions of the parameters Ω_a, Ω_b, Ω_c, Ω_d are:

$$\Omega_a = (1-B)^3; \quad \Omega_b = Z_c - B; \quad \Omega_c = (1-B)^2(B-0.25);$$
$$\Omega_d = Z_c - 0.5(1-B) \quad (9)$$

$$B = \frac{1+C_1}{\alpha_c + C_1} \qquad \alpha_c - \text{Riedel's criterion} \quad (10)$$

$$\alpha_c = 5.808 + 4.93\omega \quad (11)$$

As pointed out previously [1] the cubic GEOS equation is a general form for all the cubic equations of state with two, three and four parameters. This is the meaning of the statement cubic "general equation of state" used for GEOS.

As shown in our previous paper [1], to obtain the parameters of the Soave-Redlich-Kwong (SRK) equation of state from the equation (1) we set the following restrictions: $\Omega_c = -(\Omega_b/2)^2$ and $\Omega_d = -\Omega_b/2$. It follows:

$$\Omega_c = (1-B)^2(B-0.25) = -(Z_c - B)^2/4$$
$$\Omega_d = Z_c - 0.5(1-B) = -(Z_c - B)/2 \quad (12)$$

It results Z_c (SRK) = 1/3, and the relation for B(SRK):

$$B = 0.25 - \frac{1}{36}\left(\frac{1-3B}{1-B}\right)^2 \quad (13)$$

Solving iteratively this equation gives B(SRK)= 0.2467, and correspondingly: Ω_a(SRK) = (1-B)^3 = 0.42748 and Ω_b(SRK) = Z_c - B = 0.08664.

For Peng-Robinson (PR) equation of state we set the restrictions: $\Omega_c = -2(\Omega_b)^2$ and $\Omega_d = -\Omega_b$. It results:

$$B = 0.25 - \frac{1}{8}\left(\frac{1-3B}{1-B}\right)^2; \qquad Z_c = \frac{1+B}{4} \quad (14)$$

giving B(PR) = 0.2296 and Z_c(PR) = 0.3074.

The TBS EOS results from the following conditions:

$$\Omega_c = (1-B)^2(B-0.25) = -B_cC_c - \frac{(B_c+C_c)^2}{4} - D_c^2 \quad (15)$$

$$\Omega_d = Z_c - (1-B)/2 = -(B_c + C_c)/2 \quad (16)$$

giving, for optimized Z_c (TBS) and D_c (TBS) parameters, the equation of the B (TBS):

$$B = 0.25 + \frac{1}{(1-B)^2}\left[(Z_c - B)(3Z_c - 1) - (Z_c - \frac{1-B}{2})^2 - D_c^2\right] \quad (17)$$

The C1 EOS results from the following conditions:

$$\Omega_a^{1/3} = (1-B) = \Omega_{C1} = 0.77; \qquad B = 0.23; \quad (18)$$

$$\Omega_b = Z_c - B = Z_c - 0.23$$
$$\Omega_c = -(\Omega_{r1} - \Omega_{r2})^2/4 = (1-B)^2(B-0.25) \quad (19)$$

$$\Omega_d = (\Omega_{r1} + \Omega_{r2})/2 = Z_c - (1-B)/2 \quad (20)$$

with Ω_{r1} and Ω_{r2} parameters of C1 EOS.

The equations for B can be solved iteratively, starting with a initial approximation of B in the right hand term. For all EOSs the corresponding value for Ω_a, Ω_b, Ω_c, Ω_d are given by equations (9-10).

Results and discussions

In order to calculate the phase equilibrium and the thermodynamic properties for R23 the following equations of state have been used: Soave-Redlich-Kwong (SRK), Peng-Robinson (PR), Trebble-Bishnoi-Salim (TBS), Freze et al (C1), and GEOS3C.

The investigated *PVT* range covers single-phase (liquid or gas) and two-phase (liquid-vapour) regions, using recommended NIST data as pseudo-experimental values.

Component	C_1	C_2	C_3	T_c (K)	P_c (bar)	Z_c	ω
R23	0.2989	0.6897	-0.5128	299.29	48.32	0.2581	0.2630

Table 1
VALUES OF C_1, C_2, C_3 PARAMETERS FOR R23. CRITICAL DATA AND ACENTRIC FACTOR FROM NIST DATABASE [21]

The calculations were made with the software package PHEQ (Phase Equilibria) developed in our laboratory [28].

Using NIST values of the critical constants and the acentric factor for the calculation of α_c from the equation (11), the C_1, C_2 and C_3 parameters were obtained by constraining the equation of state to reproduce the NIST vapour pressure data and liquid volumes on the saturation curve.

The values of C_1, C_2, C_3 parameters for the GEOS3C equation, the critical data and acentric factor for R23 are given in table 1.

The following thermodynamic properties have been predicted: compressibility factor (*Z*), enthalpy (*H*), enthalpy of vaporization ($\Delta^v H$), entropy (*S*), heat capacity at constant pressure (C_P), heat capacity at constant volume (C_V), heat capacity ratio (C_P/C_V), speed of sound (*Ws*), fugacity coefficient (φ), Joule-Thomson coefficient, (*JT*). No data on these thermodynamic properties were used in this work to obtain the GEOS3C parameters.

In tables 2-4 the average absolute deviations (AAD), between calculated values by EOSs and NIST recommended data are reported for refrigerant R23.

For each table the number of data points, the pressure and temperature ranges are indicated. The two-phase region properties have been calculated at temperatures from the triple point to the critical point.

The average absolute deviations for a property *Y* are relative (%):

$$\text{AAD \%} = \frac{\sum_{i=1}^{N} \left| (Y_i^{eos} - Y_i^{exp}) / Y_i^{exp} \right| \cdot 100}{N} \quad (21)$$

excepting the enthalpy and entropy where:

$$\text{AAD } H \text{ (or } S) = \frac{\sum_{i=1}^{N} \left| H_i^{eos} - H_i^{exp} \right|}{N} \quad (22)$$

As can be seen in table 2, the vapour pressure and liquid and vapour saturated volumes are better reproduced by GEOS3C, compared to the results obtained using other equations. The liquid volumes calculated with the SRK, C1 and PR equations have large average deviations in comparison with experimental data (21.6, 8 and 6.2 %). The vapour volumes are satisfactorily predicted by all equations of state, excepting SRK.

All EOSs predict well the enthalpies and the entropies on the saturation curve and also the enthalpy of vaporization.

The GEOS3C and TBS equations predict better the liquid heat capacity, the liquid heat capacity ratio, vapour speed of sound and liquid *JT* coefficient in the saturation range, but the liquid speed of sound deviations are higher for these equations in comparison with SRK, PR, and C1. The AAD% given in table 3 for the *JT* coefficients in the saturated liquid range are relatively high, determined by very small values ($\sim 10^{-4}$) of the NIST *JT* coefficients at temperatures where the function changes the sign.

The difference in predictions between the EOSs is less noticeable for all thermodynamic properties in the single phase region (table 4) excepting speed of sound.

In this case, the SRK, PR, and C1 equations predict better values in comparison with TBS and GEOS3C. The speeds of sound values in liquid phase and in single-phase region, predicted by GEOS3C, have large deviations in comparison with NIST recommended data. The value of W_s (speed of sound) is dependent of both heat capacity ratio and the derivative $\left(\frac{\partial P}{\partial V}\right)_T$. The GEOS3C equation predicts reasonable the heat capacity ratio, but the derivative $\left(\frac{\partial P}{\partial V}\right)_T$ has higher deviations relative to NIST equation of state [29].

Representative examples of calculated properties in comparison with NIST data are provided in the figures 1-

	AAD (%)				AAD			
EOS	P^S	V^L	V^V	$\Delta_{vap}H$	H^L (kJ/kg)	H^V (kJ/kg)	S^L (kJ/kg/K)	S^V (kJ/kg/K)
SRK	3.10	21.6	5.75	3.50	7.10	2.01	0.02	0.01
PR	1.12	8.04	2.87	2.67	4.49	1.87	0.02	0.01
C1	1.98	6.33	3.82	2.99	4.71	2.05	0.02	0.01
TBS	1.01	4.24	2.35	2.35	6.26	3.51	0.02	0.01
GEOS3C	0.16	4.19	1.83	2.65	7.77	6.26	0.03	0.02

Table 2
PVT AND THERMODYNAMIC FUNCTION DEVIATIONS ON THE SATURATION CURVE FOR **R23**. TEMPERATURE RANGE (K): 118.02 – 299.29. PRESSURE RANGE (bar): 0.00058 – 48.317. NUMBER OF DATA POINTS: 41.

	AAD (%)							
EOS	C_P^L	C_P^V	$(C_P/C_V)^L$	$(C_P/C_V)^V$	W_S^L	W_S^V	JT^L	JT^V
SRK	13.5	22.7	17.6	3.90	10.1	4.83	158.9	41.8
PR	14.1	23.3	17.1	3.98	9.70	3.69	134.9	41.7
C1	14.0	23.3	17.3	4.02	13.1	3.41	165.4	41.4
TBS	9.3	24.3	14.7	4.40	32.7	2.08	64.9	41.3
GEOS3C	10.8	24.6	12.3	5.49	47.0	2.54	94.3	41.3

Table 3
THERMODYNAMIC FUNCTION DEVIATIONS AT SATURATION FOR **R23**. TEMPERATURE RANGE (K): 118.02 – 299.29. PRESSURE RANGE (bar): 0.00058 – 48.317. NUMBER OF DATA POINTS: 40

	AAD		AAD (%)				
EOS	*S* kJ/kg/K	*H* kJ/kg	*Z*	C_P	W_S	C_P/C_V	*JT*
SRK	0.02	4.85	7.05	4.09	3.28	4.35	31.9
PR	0.02	4.66	1.83	5.12	4.02	3.83	32.0
C1	0.02	4.74	2.44	4.94	4.76	3.86	36.3
TBS	0.03	6.93	2.51	3.55	16.5	4.92	30.8
GEOS3C	0.03	9.62	2.47	5.71	22.8	4.15	32.6
GEOS3C*	0.04	10.1	2.85	5.28	23.2	5.73	36.8

GEOS3C* - with the modified temperature function, eq. (5)

Table 4
THERMODYNAMIC FUNCTION DEVIATIONS ON ISOTHERMS IN SINGLE-PHASE REGION FOR **R23**. TEMPERATURE RANGE (K): 118.02 – 475. PRESSURE RANGE (bar): 0.0001 – 1200. NUMBER OF DATA POINTS: 575.

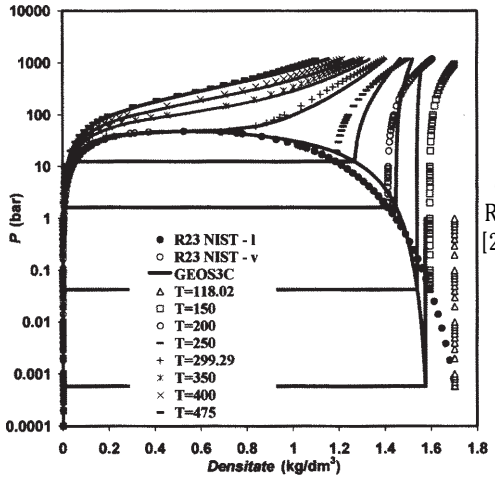

Fig. 1. Pressure – density diagram for R23. Points: NIST data [21]. Lines: prediction with the GEOS3C equation.

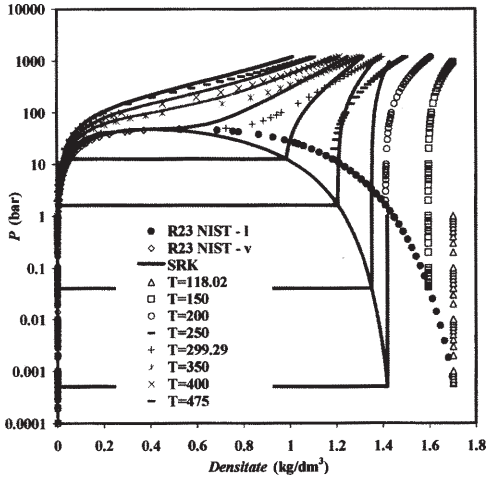

Fig. 2. Pressure – density diagram for R23. Points: NIST data [21]. Lines: prediction with the SRK equation.

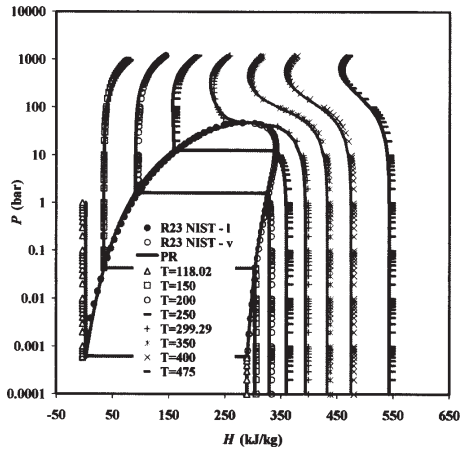

Fig.3. Pressure – enthalpy diagram for R23. Points: NIST data [21]. Lines: prediction with the PR equation

10. Figures 1 and 2 depict pressure – density diagrams for R23. Points figure NIST data, while the curves are calculated with the GEOS3C and SRK equations, for the saturation region and subcritical and supercritical isotherms. The liquid saturated densities calculated with the GEOS3C equation are in better agreement with the experimental data (NIST), in comparison with the densities calculated by the SRK equation. As pointed out already, liquid saturated densities have been used for the C_1, C_2 and C_3 parameter fitting of GEOS model. A similar fitting for SRK or PR equations does not improve the liquid densities, a translation in volume being necessary. For TBS EOS we used the generalization equations of their adjustable parameters.

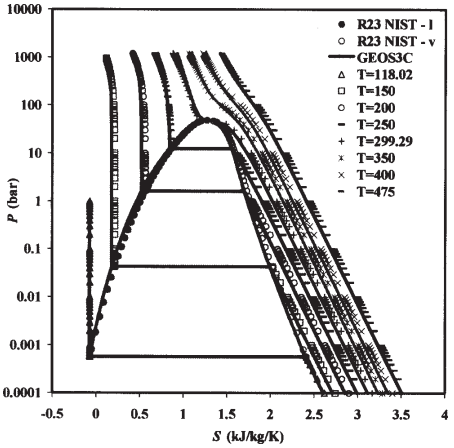

Fig. 4. Pressure – entropy diagram for R23. Points: NIST data [21]. Lines: prediction with the GEOS3C equation.

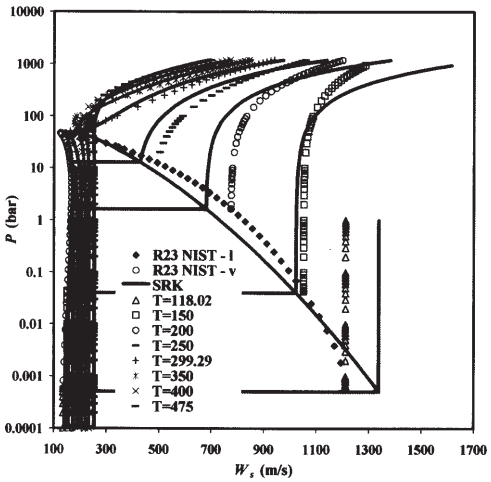

Fig. 5. Pressure – speed of sound diagram for R23. Points: NIST data [21]. Lines: prediction with the SRK equation

The calculated enthalpies and entropies with PR and GEOS3C equations, on the saturation curve and in the single phase region, are shown in figure 3 and figure 4 (points: NIST recommended data). Both models under consideration yield comparable accuracy in predicting enthalpies and entropies.

The figure 5 shows the pressure – speed of sound diagram predicted by SRK equation for R23, in the entire range of T and P. The predicted values of this equation are in better agreement with the NIST data (see tables 3-4).

The pressure-isobaric heat capacity diagram (saturation curve and several isotherms) of R23 is presented in figure 6. Points figure NIST data while the curves are calculated with the TBS equation and are in good agreement with NIST recommended data.

In the NIST data base [21] there are available isobaric properties of pure fluids. It is of interest to see the quality of predictions of thermodynamic properties in isobaric conditions. The temperature–compressibility factor (Z) and temperature–isobaric heat capacity diagrams for R23 (saturated phases and isobars) predicted by GEOS3C equation are plotted in figure 7 and 8 (points represent NIST data). The predicted properties are of same accuracy as those obtained for isotherms. Moreover, the GEOS3C predictions reproduce the pattern of properties in isobaric diagrams, for example the enthalpy and compressibility factor on isobars crossing the saturated range.

In the figure 8, the discontinuities in the isobaric heat capacity predicted by GEOS3C equation are shown on the isobars of 80, 400, 1200 bar. These discontinuities were eliminated by using the GEOS3C* equation, figure 9, with the modified temperature function, eq. (5).

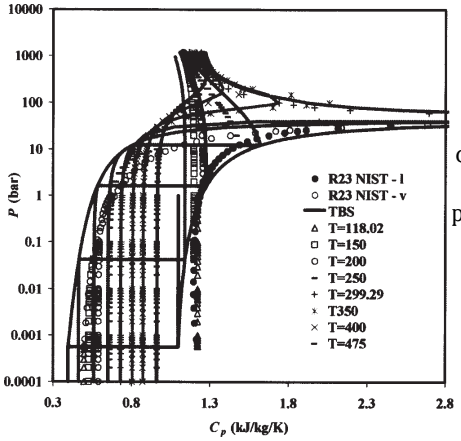

Fig.6. Pressure – isobaric heat capacity diagram of R23. Points: NIST data [21]. Lines: prediction with the TBS equation

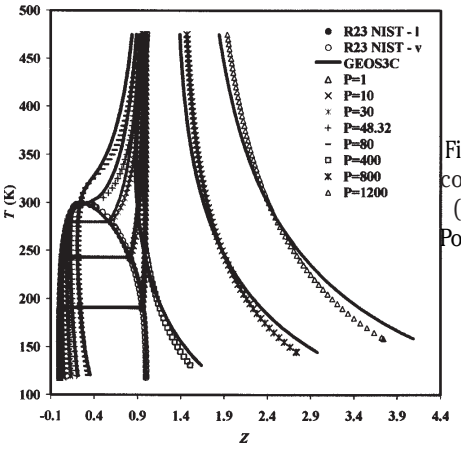

Fig.7. Temperature – compressibility factor (Z) diagram of R23. Points: NIST data [21]. Lines: prediction with the GEOS3C equation

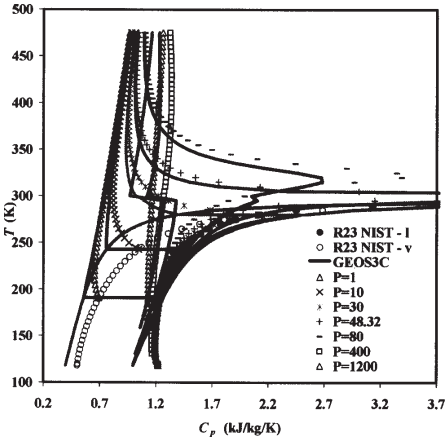

Fig.8. Temperature – isobaric heat capacity diagram of R23. Points: NIST data [21]. Lines: prediction with the GEOS3C equation

In the NIST data base [21] there are also available isochoric properties of pure fluids. It is of interest to see the quality of predictions of thermodynamic properties with cubic EOSs in isochoric conditions. Some authors [30, 31] have presented calculations with cubic EOSs for isochoric conditions. The cubic EOSs have the restriction to be applicable only for specific volumes $V > b$. Each cubic equation of state has its covolume value. For the cubic EOSs used in this paper the values of covolume are given in table 6. As can be seen, the C1 EOS has the lowest covolume value, and the SRK EOS the highest values. In consequence, the calculation of a isochore of $V = 0.52$ dm^3/kg is possible with C1 EOS, but not with the other four equations.

Figure 10 shows the pressure – temperature diagram with isochors predicted by the original GEOS3C and the modified GEOS3C* equations. The isochors in the vapor region (at $V > V_c$) are very good predicted by the both versions GEOS3C, in good agreement with NIST data. The agreement with NIST data is reasonably good for the critical

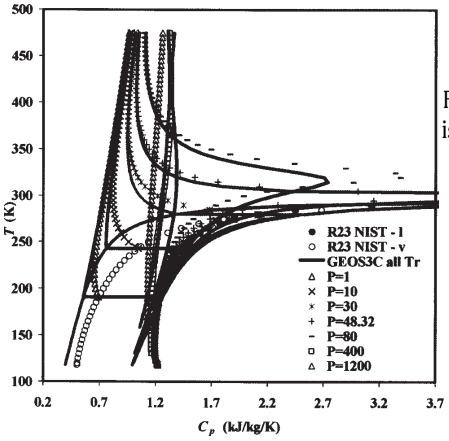

Fig. 9. Temperature – isobaric heat capacity diagram of R23. Points: NIST data [21]. Lines: prediction with the GEOS3C* equation (5)

Table 6

VALUES OF b PARAMETER OF CUBIC EOS's FOR **R23**

EOS	SRK	PR	C1	TBS	GEOS3C
b, dm^3/kg	0.6374	0.5723	0.5081	0.6212	0.6085

isochore. Deviations in GEOS3C predictions from the NIST data are higher in the liquid region, and rise when the isochors are calculated at specific volumes $V'!b$. This behaviour is similarly for all cubic EOS's. The deviations of the predictions on the isochore of $V = 0.62$ dm^3/kg are very large, and surely not recommended to be used in applications. The two versions GEOS3C (lines) and the modified GEOS3C* (dotted lines) perform similarly, and when the same values of properties are obtained only the lines of GEOS3C are depicted.

The temperature – entropy diagram (saturation curve and several isochors) of R23 is presented in figure 11. Points figure NIST data while the curves are calculated with the the original GEOS3C and the modified GEOS3C* equations. The agreement with NIST data is reasonably good, excepting the range at specific volumes $V'!b$. A good

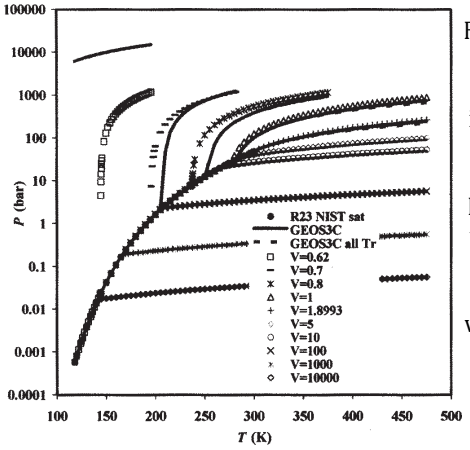

Fig. 10. Pressure – temperature diagram with isochors for R23. Points: NIST data [21]. Lines: prediction with the GEOS3C equation. Dotted lines: prediction with the GEOS3C* equation (5).

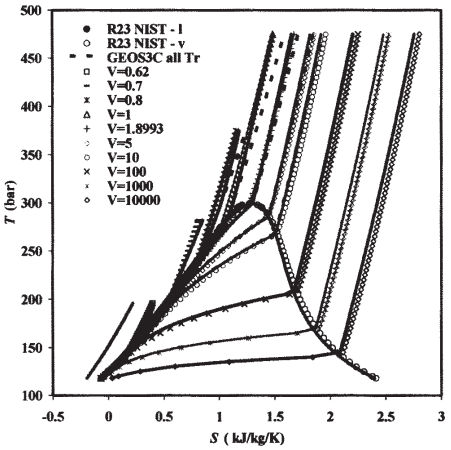

Fig. 11. Temperature – entropy diagram (saturation curve and several isochors) for R23. Points: NIST data [21]. Lines: prediction with the original GEOS3C equation. Dotted lines: prediction with the GEOS3C* equation (5).

agreement of the GEOS3C predictions with NIST data is to be observed for parts of the isochors situated in the vapour-liquid range. Again the two versions GEOS3C (lines) and the modified GEOS3C* (dotted lines) perform similarly, and when the same predictions are obtained only the lines of GEOS3C are depicted.

Conclusions

The vapour-liquid equilibrium and the thermodynamic properties of refrigerant R23 were predicted by five cubic equations of state SRK, PR, TBS, C1 and GEOS3C on a wide *PVT* range, including the entire saturation region. A large comparison with recommended NIST data was made.

The following thermodynamic properties were calculated: compressibility factor, *Z*; enthalpy, *H*; enthalpy of vaporization, $\Delta^{v}H$; entropy, *S*; heat capacity at constant pressure, C_p; heat capacity at constant volume, C_V; heat capacity ratio, C_P/C_V; speed of sound, *Ws*; fugacity coefficient, *j*; Joule-Thomson coefficient, *JT*.

The GEOS3C equation gives better predictions of vapour pressure and saturated liquid volume than the other equations of state. The saturated vapour volume is well reproduced by all equations of state. All EOSs predict well the enthalpies and the entropies on the saturation curve and also the enthalpy of vaporization. The GEOS3C and TBS equations predict better the liquid heat capacity, the liquid heat capacity ratio and liquid JT coefficient in the saturation range but the liquid speed of sound deviations are higher for these equations in comparison with SRK, PR, and C1.

The difference in predictions between the EOSs is less noticeable for all thermodynamic properties in the single phase region excepting speed of sound. In this case, the SRK, PR, and C1 equations predict better values in comparison with TBS and GEOS3C.

This study shows that the cubic EOSs lead to reasonable predictions of VLE and thermodynamic properties of R23, resting simple enough for applications in chemical engineering.

The GEOS3C equation has some advantages, notably being a general form for all the cubic equations of state with two, three and four parameters proposed in the literature. A slightly modification of the temperature function in its cohesive term solves the problem of discontinuity in some thermodynamic properties at critical temperature of the pure fluids.

List of symbols

a, b, c, d - parameters in GEOS3C
AAD- absolute average deviation
B- dimensionless parameter in GEOS3C, defined by eq. (7)
C_1, C_2 and C_3- parameters in GEOS3C temperature function
C_V, C_p- isochoric and isobaric heat capacities
EOS- equation of state
H- enthalpy
JT- Joule-Thomson coefficient
M- molar mass
P, P^s- pressure, saturation pressure
R- universal gaz constant
S- entropy
T- temperature
V, V^L, V^V- molar volume, liquid volume, vapor volume
*W*s- speed of sound
Y- thermodynamic function (general notation)
Z- compresibility factor

Greeks

α_c- Riedel's criterium (parameter in GEOS3C)
β - reduced temperature function in GEOS3C
φ *j*- fugacity coefficient
Ω_a, Ω_b, Ω_c, Ω_d - parameters of GEOS3C
ω- acentric factor

Subscripts

c- critical property
r- reduced property

References

1. GEANĂ D., FEROIU V., Fluid Phase Equilibria, 174, 2000, p. 51.
2. VALDERRAMA J.O., Industrial Engineering Chemical Research, 42, 2003, p. 1603.
3. VALDERRAMA J.O., ZAVALETA J., Fluid Phase Equilibria, 234, 2005, p. 136.
4. ANDERKO A, Cubic and generalized van der Waals equations, in: J.V. Sengers, R.F. Kayser, C.J. Peters, H.J. White Jr. (Eds.), Equations of State for Fluids and Fluid Mixtures. Elsevier, Amsterdam **2000**, *Part I*, p. 75–126.
5. POLISHUK I., WISNIAK J.; SEGURA H., Chemical Engineering Science, 56, 2001, p. 6485.
6. POLISHUK I., WISNIAK J.; SEGURA H., Fluid Phase Equilibria, 164, 1999, p. 13.
7. WERTHEIM M. S., J. Stat. Phys, 35, 1984, p. 19 and p. 35.
8. WERTHEIM M. S., J. Stat. Phys, 42, 1986, p. 459 and p. 477.
9. CHAPMAN W. G., GUBBINS K. E., JACKSON G., RADOSZ M., Fluid Phase Equilibria, 52, 1989, p. 31.
10. CHAPMAN W. G., GUBBINS K. E., JACKSON G., RADOSZ M., Industrial Engineering Chemical Research, 29**,** 1990, p. 1709.
11. KONTOGEORGIS G. M., VOUTSAS E. C., YAKOUMIS I. V., TASSIOS D. P., Industrial Engineering Chemical Research., 35, 1996, p. 4310.
12. MULLER E.A., GUBBINS K.E., Industrial Engineering Chemical Research, 40, 2001, p. 2193.
13. KONTOGEORGIS G.M., FOLAS G.K., Thermodynamic Models for Industrial Applications. From Classical and Advanced Mixing Rules to Association Theories, John
Wiley & Sons Ltd., New York, 2010.
14 POLISHUK I., Fluid Phase Equilibria, 298, 2010, p. 67.
15. PRIVAT R., GANI R., JAUBERT J.-N., Fluid Phase Equilibria, 295, 2010, p. 76.
16. JAUBERT J.-N., MUTELET F., Fluid Phase Equilibria, 224, 2004, p. 285.
17. JAUBERT J.-N., PRIVAT R., Fluid Phase Equilibria, 295, 2010, p. 26.
18. JAUBERT J.-N., PRIVAT R., MUTELET F., AIChE J.**,** 56(12), 2010, p. 3225.
19. GEANĂ D., Proc.Rom.Acad.,Series B, 1-2, 2003, p. 3. and 1, 2005, p. 9.
20. POLISHUK I., Industrial Engineering Chemical Research, 50, 2011, p. 4183.
21.*** NIST - Thermophysical Properties of Fluid Systems, Database 2010, http://webbook.nist.gov/chemistry/fluid/.
22. SOAVE G., Chem. Eng. Sci., 27, 1972, p. 1197.
23. PENG D. Y., ROBINSON D. B., Ind. Eng. Chem. Fundam., 15, 1976, p. 59.
24. SALIM P. H., TREBBLE M. A., Fluid Phase Equilibria, 65, 1991, p. 59.
25. FREZE R., CHEVALIER J.-L., PENELOUX A., RAUZY E., Fluid Phase Equilibria, 15, 1983, p. 33.
26. GEANĂ D., FEROIU V., Proceedings of the National Conference on Chemistry and Chemical Engineering, Bucharest, Romania, oct. 1995, vol. 3, p. 133.
27. NOUR M., DUNĂ D., IONITĂ M., FEROIU V., GEANĂ D., U.P.B. Sci. Bull., Series B, 2013, in print.
28. GEANĂ D., RUS L., Proceeding of the Romanian International Conference on Chemistry and Chemical Engineering (RICCCE XIV), Bucharest, Romania, oct. 2005, vol. 2, p. 170; www.chfiz.pub.ro/laboratories/trl/myweb/termod.
29. NOUR, M., DUNĂ, D., IONITĂ, M., FEROIU, V., GEANĂ, D., Rev. Chim. (Bucharest), **64**, no. 10, 2013, p. 1055.
30. MARTIN J. J., Ind. Chem. Eng. Fundam., 18, 1979, p. 81.
31. GEANĂ D., Rev. Chim. (Bucharest), **37**, no. 4, 1986, p. 303.

Manuscript received: 3.03.2014